Appl. Phys. B 74, 741–744 (2002)
DOI: 10.1007/s00340-002-0926-4

Applied Physics B
Lasers and Optics

O. NEY[1]
M. TRZECIECKI[1,2]
W. HÜBNER[1,✉]

Femtosecond dynamics of spin-dependent SHG response from NiO (001)

[1] Max-Planck-Institut für Mikrostrukturphysik, Weinberg 2, 06120 Halle, Germany
[2] Institute of Physics, Warsaw University of Technology, Koszykowa 75, 00-662 Warsaw, Poland

Received: 16 October 2001/Revised version: 21 March 2002
Published online: 6 June 2002 •

ABSTRACT Based on a parameterized electronic many-body theory we calculate the spectrum of optical second-harmonic generation (SHG) on an antiferromagnetic (AF) surface: NiO (001). The occurrence of AF spectral lines is further exploited for the calculation of ultra-fast spin dynamics. This spin dynamics is observable in SHG. It is characterized by both a sharp drop of the AF signal within a few femtoseconds and a long persistence (up to nanoseconds) of the spin coherence. These two features constitute an ideal system for possible applications in both magnetic recording and quantum computing.

PACS 78.47.+p; 75.50.Ee; 78.20.Ls; 75.10.Dg

1 Introduction

The current speed of magnetic recording is of the order of nanoseconds, i.e.close to a single precession cycle of the magnetization (Larmor frequency). Achieving a higher speed will require completely new approaches, such as hybrid or optical recording. In order to overcome the deficiencies of the contemporary computer memories, both permanent and dynamic, new designs like magnetic random access memories (MRAMs) are under development [1]. They will eliminate the mechanical motion and the hierarchical structure of the contemporary memories and simplify the design of CPUs. One of the most important components of these MRAMs are tunneling magnetoresistance (TMR) devices, where the read-out current passing through the device depends on the relative magnetization of two ferromagnetic layers. The central layer of this trilayer structure consists of an oxide sandwiched between a soft and a hard magnetic layer (often a ferro-/antiferromagnetic exchange-bias system). Therefore, the performance of these future devices depends heavily on the properties of oxides, which may be nonmagnetic or antiferromagnetic (AF). Besides, the spin dynamics of oxide surfaces may be interesting in itself. We find that a cubic antiferromagnet such as NiO may have the features perfectly suitable for these purposes, since it presents fast dynamics and long-lived coherence.

Optical second-harmonic generation (SHG) has been proven to be a versatile technique for the investigation of ferromagnetism at surfaces. The sensitivity of this technique to volume antiferromagnetism has been shown experimentally [2] and explained theoretically [3]. The sensitivity of SHG to surface antiferromagnetism has been predicted theoretically [4, 5]. Only very recently, seminal experimental work has been performed in the sub-picosecond regime for ferromagnetic materials [6–10], where the spin–lattice relaxation processes [11] cannot be responsible for the observed effect. A proper model, dynamics of complex populations, has been developed for both linear [12] and nonlinear [13] magneto-optics from ferromagnets. Recently, even the laser control of ferromagnetism has been predicted theoretically [14]. However, the investigation of femtosecond spin dynamics of antiferromagnets is still in its infancy.

Here, we describe the electronic theory of a pump-and-SHG-probe experiment on NiO (001). During such an experiment, the sample is excited by a strong laser pulse, and then (with a variable delay of several tens to hundreds of femtoseconds) the second – probe – pulse is issued. The SHG response of the excited sample to this second pulse is monitored and can reveal the dynamic properties of the sample.

2 Theory

The description of time-dependent magnetic effects encountered in transition metals and their oxides requires the proper treatment of correlation effects. While they are important even in some effects of the ground state [15], their relevance is evident in nonlinear optics where highly excited states are frequently involved. Therefore, we employ an exact-diagonalization method which allows for a nonperturbative treatment of electronic correlation in the crystal field [16]. Under these conditions, the most general Hamiltonian is of the following form:

$$H = H_{\text{band}} + H_{\text{C}} + H_{\text{SO}}, \tag{1}$$

where H_{band} describes the band structure of the investigated system, H_{C} describes the on-site Coulomb interaction, and H_{SO} is the relativistic part, which describes the spin–orbit coupling needed for magneto-optics. We neglect H_{band}, since we focus on the low-energy spectrum resulting from the atomic multiplet states within the bulk gap of NiO. In this work, we use an on-site interaction part of the Hamiltonian, which is of the following form:

$$H_{\text{C}} = \sum_{i,j,k,l,\sigma,\sigma',\sigma'',\sigma'''} U_{i\sigma,j\sigma',l\sigma''',k\sigma''} c^{\dagger}_{i\sigma} c^{\dagger}_{j\sigma'} c_{k\sigma''} c_{l\sigma'''}. \tag{2}$$

✉ Fax: 49-345/5511-223, E-mail: huebner@mpi-halle.de

Here, $U_{i\sigma,j\sigma',l\sigma''',k\sigma''}$ is the on-site Coulomb interaction, which can be described in full generality by three parameters: the Coulomb repulsion U, the exchange interaction J, and the exchange anisotropy ΔJ. $c_{i\sigma}^{(\dagger)}$ destroys (creates) a hole of spin σ in d-orbital i. In this section, we will concentrate on this on-site Hamiltonian, which possesses the full spherical symmetry of a free Ni ion. The assumption is that exactly two electrons are transferred to the oxygen atom, so that the electronic configurations of the Ni^{2+} ion are $3d^8 4s^0$, $3d^7 4s^1$, or $3d^6 4s^2$, while the parameter U determines the energy separation between these states. The energy difference between the configurations $3d^8 4s^0$ and $3d^7 4s^1$ constitutes the gap of around 4.0 eV, which makes NiO a charge-transfer insulator. The states most interesting to us are the 8-, 7-, or 6-electron states of the d-shell or, equivalently, the 2-, 3-, or 4-hole states of the d-shell of the Ni ion. Two- and three-hole states for a Ni atom have been derived in [17]. By the inclusion of the four-hole states we arrive at a reliable theory that allows us to treat, for example, AF CoO and FeO surfaces also. For simplicity, we restrict ourselves in this paper to two-hole states.

This Hamiltonian allows for the determination of the many-body states of a free Ni ion by coupling of single-hole states according to the Clebsch–Gordan algebra [16]. As the Hamiltonian possesses the full spherical symmetry, these states are highly degenerate. These degeneracies are partially lifted by the crystal field and further by the surface. Due to the sensitivity of nonlinear magneto-optic effects to the splitting of electronic levels [18], we examine this splitting carefully. Level splitting due to lowering of the symmetry is governed by group theory. In particular, it tells us that, for cubic symmetry O_h (surface square symmetry C_{4v}), only representations of the order up to three (two) are possible. These conditions fix the maximum orbital degeneracies. The energy levels corresponding to the surface states are then determined by a ligand-field approach. We fit the ligand-field parameters according to the energy levels observed experimentally [19], and use these parameters to obtain the energy levels of all the states at NiO (001). The two-hole states and their energies, as well as the description of the states in terms of ligand-field parameters, are presented in Table 1 [20].

The time-resolved evolution of the states resulting from the described procedure gives rise to a time-dependent nonlinear optical response. This response is described (within the electric-dipole approximation) by the nonlinear susceptibility tensor $\chi^{(2\omega)}(t)$, which according to [13, 21, 22] can be described as[1]

$$\chi^{(2\omega)}_{\alpha\beta\gamma}(t) \sim \sum_{\boldsymbol{k},l,l',l''} \Bigg[\langle \boldsymbol{k}, l''|\boldsymbol{r_\alpha}|\boldsymbol{kl}\rangle \langle \boldsymbol{kl}|\boldsymbol{r_\beta}|\boldsymbol{k}, l'\rangle \langle \boldsymbol{k}, l'|\boldsymbol{r_\gamma}|\boldsymbol{k}, l''\rangle \times \frac{\frac{p(E_{\boldsymbol{k},l''},t)-p(E_{\boldsymbol{k},l'},t)}{E_{\boldsymbol{k},l''}-E_{\boldsymbol{k},l'}-\hbar\omega+\mathrm{i}\hbar\alpha} - \frac{p(E_{\boldsymbol{k},l'},t)-p(E_{\boldsymbol{kl}},t)}{E_{\boldsymbol{k},l'}-E_{\boldsymbol{kl}}-\hbar\omega+\mathrm{i}\hbar\alpha}}{E_{\boldsymbol{k},l''}-E_{\boldsymbol{kl}}-2\hbar\omega+2\mathrm{i}\hbar\alpha} \Bigg], \quad (3)$$

where $p(E_{\boldsymbol{kl}}, t) = \langle\Psi(t)|\boldsymbol{kl}\rangle = f(E)\mathrm{e}^{-(\mathrm{i}/\hbar)E_{\boldsymbol{k},l}t}$ are time-dependent populations, $\boldsymbol{r}_\alpha$ ($\alpha = x, y, z$) is the α-component of the electric-dipole operator, and f is the Fermi distribution. The summation is over wave vectors $\boldsymbol{k}$, the states l, l', and l'', and also over two lattice sites, with the atomic magnetic moments set antiparallel in the AF phase (staggered summation). This allows us to account for the antiferromagnetism. The damping factor α gives the causal part of the Green's function and corresponds to the breaking of time-reversal symmetry of the Hamiltonian. The matrix elements $\langle \boldsymbol{k}, l|i,\ j,\ \text{or}\ k|\boldsymbol{k}, l\rangle$ describe transitions between the electronic d and s states of Ni; consequently they are forbidden in the spherically symmetric environment. Breakdown of the inversion symmetry at the surface changes the selection rules, so that transitions with $\Delta l = \pm 2, \pm 1$, and 0 are allowed. We restrict ourselves to intra-atomic transitions, since they suffice to explain the spectral structures within the gap of NiO (001) [23, 24]. We also do not have to resort to the interplay of electric- and magnetic-dipole effects – the electric-dipole approximation is sufficient to explain all the mentioned magneto-optical effects on NiO (001), including the AF domain imaging [4]. In order to improve this approximation an explicit calculation of the transition-matrix elements will be performed. This, however, is beyond the scope of the current paper.

[1] ω is a fundamental probe frequency.

Free-ion state	Surface state	Ligand-field correction	Energy (eV)
^1S	$^1A_1$	$2\varepsilon_0$	7.9310
^3P	$^3A_2$	$2\varepsilon_0 + \frac{14}{5}D_S$	2.9738
	^3E	$2\varepsilon_0 - \frac{7}{5}D_S$	3.0099
^1D	$^1A_1$	$2\varepsilon_0 + \frac{6}{7}D_S + \frac{24}{7}D_q$	2.5363
	$^1B_1$	$2\varepsilon_0 - \frac{6}{7}D_S + \frac{24}{7}D_q + \frac{20}{7}D_U$	2.4376
	$^1B_2$	$2\varepsilon_0 - \frac{6}{7}D_S - \frac{16}{7}D_q - \frac{20}{7}D_U$	3.0125
	^1E	$2\varepsilon_0 + \frac{3}{7}D_S - \frac{16}{7}D_q$	2.8880
^3F	$^3B_1$	$2\varepsilon_0 + 12D_q + 5D_U$	0.0000
	$^3A_2$	$2\varepsilon_0 - \frac{4}{5}D_S - 6D_q$	1.3016
	$^3E_\alpha$	$2\varepsilon_0 + \frac{2}{5}D_S - 6D_q - \frac{15}{4}D_U$	1.4401
	$^3B_2$	$2\varepsilon_0 + 2D_q - 5D_U$	1.0060
	$^3E_\beta$	$2\varepsilon_0 + 2D_q + \frac{15}{4}D_U$	0.6586
^1G	$^1A_{1\alpha}$	$2\varepsilon_0 + 4D_q + \frac{5}{3}D_U$	3.4080
	$^1A_{1\beta}$	$2\varepsilon_0 + \frac{8}{7}D_S + \frac{4}{7}D_q - \frac{5}{3}D_U$	3.7393
	$^1B_1$	$2\varepsilon_0 - \frac{8}{7}D_S + \frac{4}{7}D_q + \frac{15}{7}D_U$	3.6078
	$^1A_2$	$2\varepsilon_0 + 4D_S + 2D_q$	3.5616
	^1E	$2\varepsilon_0 - 2D_S + 2D_q + \frac{5}{4}D_U$	3.5636
	$^1B_2$	$2\varepsilon_0 - \frac{8}{7}D_S - \frac{26}{7}D_q - \frac{15}{7}D_U$	4.0389
	^1E	$2\varepsilon_0 + \frac{4}{7}D_S - \frac{26}{7}D_q - \frac{5}{4}D_U$	3.9887

TABLE 1 States at the (001) surface of NiO. The ligand-field parameter ε_0 describes the energy shift in the crystal field, D_q is the level splitting in the cubic environment, and D_S and D_U correspond to the level splitting in the octahedral and C_{4v} symmetries, respectively

3 Static response of the sample

By setting the time t equal to zero and choosing ground-state occupancies in (3), we are able to study the frequency-dependent response of the sample. According to (3), there are three components needed for our calculations of the nonlinear susceptibility tensor elements: the wavefunctions of the NiO many-body eigenstates, the transition-matrix elements between these states, and the energy levels of these

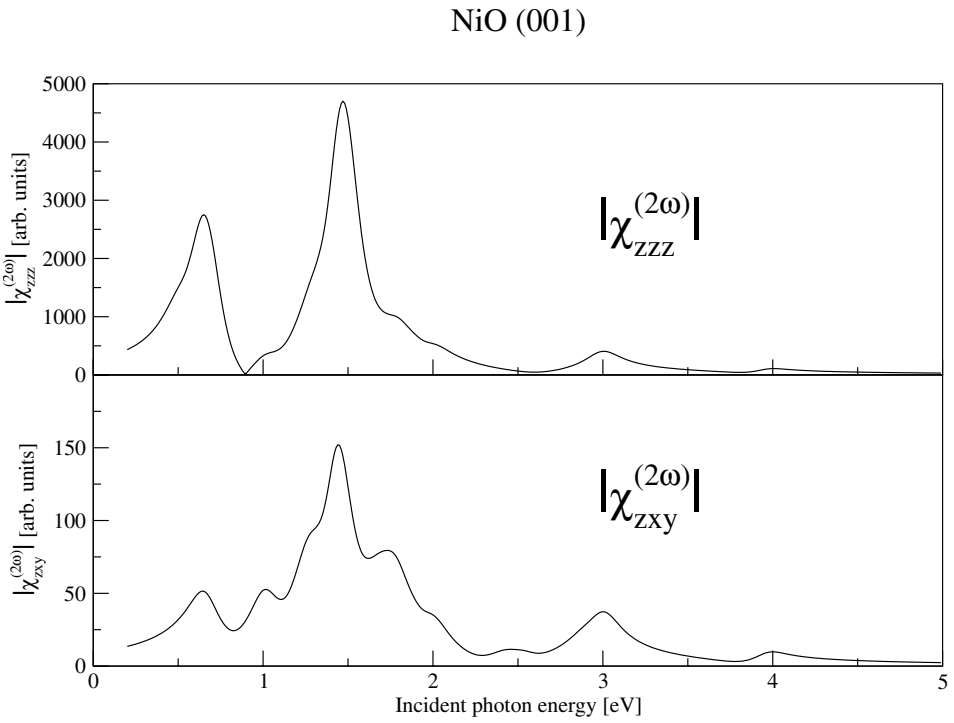

FIGURE 1 Spectra of the paramagnetic tensor element $\chi^{(2\omega)}_{zzz}$ and the antiferromagnetic tensor element $\chi^{(2\omega)}_{zyx}$

states. The wavefunctions and the corresponding energies were derived in the previous sections. However, a reliable calculation of the transition-matrix elements would require an ab initio theory of static and dynamic optical phenomena, which is not feasible so far (transition-metal oxides constitute the most difficult case due to their strong electronic correlations). Instead, we will use the approximations for the transition-matrix elements obtained by Hübner et al. [25], which constitute simple selection rules allowing for distinguishing the tensor elements.

Here, we present the spectra of two tensor elements: the prototypic paramagnetic tensor element $\chi^{(2\omega)}_{zzz}$ and the prototypic AF tensor element $\chi^{(2\omega)}_{zxy}$ in Fig. 1. In both spectra, all the features fall within the gap, which we assume at 4.0 eV. The dominant structure in both spectra corresponds to the transitions from the ground state to the states resulting from the split ^3P state, which are all located near 3.0 eV (see Table 1). The position of the peak around 1.5 eV corresponds to the fact that the tensor describes SHG. Other, smaller peaks related to transitions between various states are also present. Another feature of the calculated spectra is that the tensor elements are complex and their phases vary. This has important consequences for the AF domain imaging using SHG, as discussed in [26].

The main distinctive features of the spectrum of the AF tensor element $\chi^{(2\omega)}_{zxy}$ are additional peaks at 1.02 eV, 1.73 eV, and 2.46 eV, where at best shoulders exist in the spectrum of the paramagnetic tensor element $\chi^{(2\omega)}_{zzz}$. Consequently, this is an 'antiferromagnetic' spectral line, which we suppose is especially suitable for nonlinear magneto-optics. Note that the AF SHG tensor element $\chi^{(2\omega)}_{zxy}$ is linear in the AF order parameter. Another interesting result is that both tensor elements are of similar magnitude. This is a favorable condition for AF domain imaging. Taking into account the magnitudes of both tensor elements presented in this section, the domain contrast should be as large as in ferromagnets (where it is of the order of unity in SHG, as opposed to the small domain contrast in magneto optic Kerr effect). This large contrast provides a large driving force for the dynamics of the nonlinear magneto-optical response.

4 Dynamics

Next, we turn to the calculation of the AF spin dynamics on the femtosecond time scale. The initial excitation is assumed to be infinitesimally short in time (the excitation pulse is already completed when our dynamics starts), but its energy distribution follows a Gaussian profile, centered at 2 eV and 20-eV wide (truncated at 0 eV, so that no negative energies appear). Such a strong excitation will be distributed in a real experiment among many atoms, but here we confine it to one atom without any loss of generality. The chosen width of excitation allows us to probe the fast limit of the dynamics, since all the energy levels (including the highest) are populated and consequently all de-excitation channels are open. Restricting the Hamiltonian to electronic on-site interactions complies with this limit. The initial excitation causes a strong redistribution of charges among the energy levels, visible as a drop[2] of the observed signal compared to its value in a static experiment. The time evolution of the excited system then results from the quantum phase factors and has no classical analogue. Broadening of levels does not occur, since the many-body Hamiltonian is diagonal due to the choice of the appropriate symmetry-adapted two-hole basis.

Figure 2 shows the dynamics of the AF tensor element $\chi^{(2\omega)}_{zxy}(t)$ within the first 50 fs. Such a dynamics can be probed

[2] To a value close to zero at time $t = 0$, because all the states are nearly equally populated.

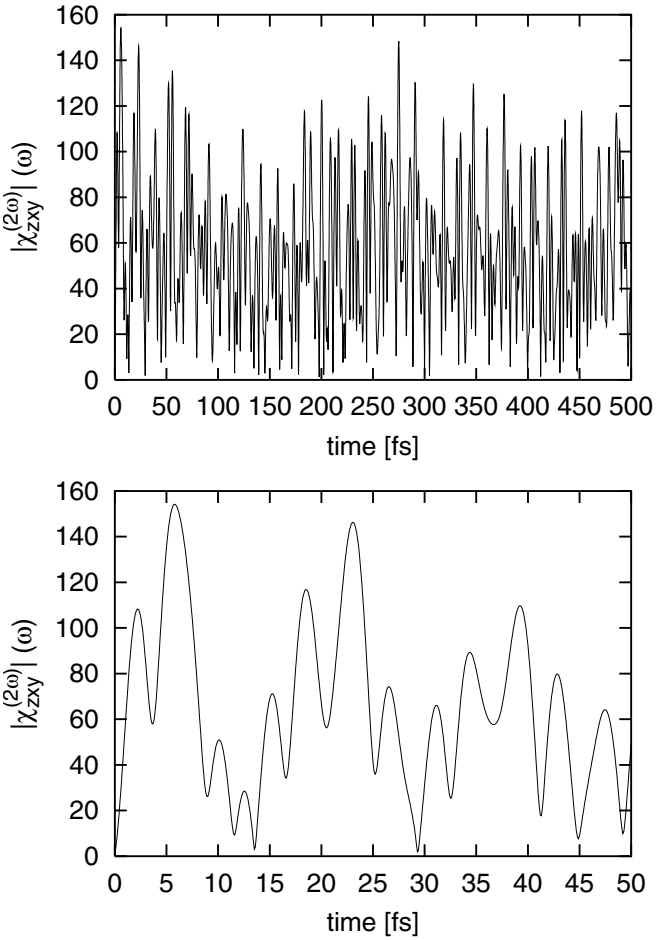

FIGURE 2 Time evolution of the tensor element $\chi^{(2\omega)}_{zyx}$ within the first 50 fs after the excitation. The *inset* shows the evolution of the same tensor element within the first 500 fs. The units are the same as in Fig. 1

in an interferometric SHG experiment. The inset shows its evolution up to 500 fs, at the fundamental photon energy 0.64 eV[3]. There is no decay of the envelope of $\chi^{(2\omega)}_{zxy}(t)$, unlike in metallic systems [13]. The coherence is preserved for a long time (until phenomena neglected here, such as electron–phonon coupling, which is of particular relevance in dielectrics, take place), which manifests itself by beats repeated regularly every 20 fs. The spin dynamics takes place within femtoseconds, thus being as fast as in metals. Consequently, we predict coherence times that are four orders of magnitude longer than the ultimate speed of the spin and charge dynamics. This allows for many read–write cycles during the intrinsic lifetime of the excitation. Besides, it fulfills one of the important conditions for quantum information [27]. This finding is in line with the experimentally determined widths of spectral lines in oxides [2] (tens of μeV, which corresponds to tens of picoseconds coherence times) and bears a similarity to the optical effects used for coherent control in semiconductor quantum dots [28].

[3] This frequency corresponds to the low-lying AF line in the SHG spectrum of NiO (001).

5 Conclusions

In this paper, we presented a study of time-resolved SHG on antiferromagnetic NiO (001). We find that the SHG spectrum exhibits AF spectral lines which show ultra-fast AF spin dynamics. This system fulfills one of the basic requirements of quantum computing, namely a high read–write speed accompanied by a long-lasting coherence. Until now, among solids, only semiconductors and nuclear spins have been known to exhibit the combination of these features, suffering however from a much slower dynamics [29]. Moreover, NiO possesses a high density of permanent magnetic moments (like metals) – an option for device-size reduction.

Note added: recent experiments by Fiebig et al. [30] for the first time showed a strongly enhanced SHG signal from antiferromagnetic bulk NiO.

REFERENCES

1 J. de Boeck, G. Borghs: Phys. World, April, 27 (1999)
2 M. Fiebig, D. Fröhlich, B.B. Krichevtsov, R.V. Pisarev: Phys. Rev. Lett. **73**, 2127 (1994)
3 V.N. Muthukumar, R. Valentí, C. Gros: Phys. Rev. Lett. **75**, 2766 (1995)
4 M. Trzeciecki, A. Dähn, W. Hübner: Phys. Rev. B **60**, 1144 (1999)
5 M. Trzeciecki, W. Hübner: Appl. Phys. B **68**, 473 (1999)
6 E. Beaurepaire, J.-C. Merle, A. Daunois, J.-Y. Bigot: Phys. Rev. Lett. **76**, 4250 (1996)
7 J. Hohlfeld, E. Matthias, R. Knorren, K.H. Bennemann: Phys. Rev. Lett. **78**, 4861 (1997); Phys. Rev. Lett. **79**, 960 (1997) (erratum)
8 A. Scholl, L. Baumgarten, R. Jacquemin, W. Eberhardt: Phys. Rev. Lett. **79**, 5146 (1997)
9 M. Aeschlimann, M. Bauer, S. Pawlik, W. Weber, R. Burgermeister, D. Oberli, H.C. Siegmann: Phys. Rev. Lett. **79**, 5158 (1997)
10 B. Koopmans, M. van Kampen, J.T. Kohlhepp, W.J.M. de Jonge: Phys. Rev. Lett. **85**, 844 (2000)
11 A. Vaterlaus, T. Beutler, F. Meier: Phys. Rev. Lett. **67**, 3314 (1991)
12 W. Hübner, G.P. Zhang: Phys. Rev. B **58**, R5920 (1998)
13 G.P. Zhang, W. Hübner: Appl. Phys. B **68**, 495 (1999)
14 G.P. Zhang, W. Hübner: Phys. Rev. Lett. **85**, 3025 (2000)
15 P. Fulde: *Electron Correlation in Molecules and Solids*, 3rd edn. (Springer, Heidelberg 1995); J. Wahle, N. Blümer, J. Schlipf, K. Held, D. Vollhardt: Phys. Rev. B **58**, 12 749 (1998)
16 M. Trzeciecki: 'Second Harmonic Generation from Antiferromagnetic Interfaces', PhD Thesis, Martin-Luther-Universität Halle-Wittenberg, 2000
17 W. Hübner, L.M. Falicov: Phys. Rev. B **47**, 8783 (1993)
18 A. Kirilyuk, V.V. Pavlov, R.V. Pisarev, T. Rasing: Phys. Rev. B **61**, R3796 (2000)
19 B. Fromme, M. Möller, T. Anschütz, C. Bethke, E. Kisker: Phys. Rev. Lett. **77**, 1548 (1996)
20 Note the improved energy fit and corrections of misprints compared to Table 1 in M. Trzeciecki, O. Ney, G.P. Zhang, W. Hübner: Adv. Solid State Phys. **41**, 547 (2001)
21 J. Dewitz: 'Nichtlineare Magneto-Optik an Fe Monolagen', PhD Thesis, Martin-Luther-Universität Halle-Wittenberg, 1999
22 W. Hübner, G.P. Zhang: J. Magn. Magn. Mater. **189**, 101 (1998)
23 K. Terakura, A.R. Williams, T. Oguchi, J. Kübler: Phys. Rev. Lett. **52**, 1830 (1984)
24 A. Gorschlüter, H. Merz: Phys. Rev. B **49**, 17 293 (1994)
25 W. Hübner, K.H. Bennemann, K. Böhmer: Phys. Rev. B **50**, 17 597 (1994)
26 M. Trzeciecki, W. Hübner: Phys. Rev. B **62**, 13 888 (2000)
27 D.P. DiVincenzo, D. Loss: J. Magn. Magn. Mater. **200**, 202 (1999)
28 N.H. Bonadeo, J. Erland, D. Gammon, D. Park, D.S. Katzer, D. Steel, G. Steel: Science **282**, 1473 (1998)
29 J.M. Kikkawa, D.D. Awschalom: Nature **397**, 139 (1999); Science **287**, 473 (2000)
30 M. Fiebig, D. Fröhlich, T. Lottermoser, V.V. Pavlov, R.V. Pisarev, H.-J. Weber: Phys. Rev. Lett. **87**, 137 202 (2001)